The American Journal of Pathology, Vol. 180, No. 4, April 2012

DOI: 10.1016/j.ajpath.2011.12.040

Molecular Pathogenesis of Genetic and Inherited Diseases

In Vivo Characterization of Mutant Myotilins

Etsuko Keduka,* Yukiko K. Hayashi,* Sherine Shalaby,* Hiroaki Mitsuhashi,*† Satoru Noguchi,* Ikuya Nonaka,* and Ichizo Nishino*

From the Department of Neuromuscular Research, National Institute of Neuroscience, National Center of Neurology and Psychiatry, Tokyo, Japan; and the Division of Genetics,† Children's Hospital Boston, Harvard Medical School, Boston, Massachusetts*

Myofibrillar myopathy (MFM) is a group of disorders that are pathologically defined by the disorganization of the myofibrillar alignment associated with the intracellular accumulation of Z-disk–associated proteins. MFM is caused by mutations in genes encoding Z-disk–associated proteins, including myotilin. Although a number of MFM mutations have been identified, it has been difficult to elucidate the precise roles of the mutant proteins. Here, we present a useful method for the characterization of mutant proteins associated with MFM. Expression of mutant myotilins in mouse tibialis anterior muscle by *in vivo* electroporation recapitulated both the pathological changes and the biochemical characteristics observed in patients with myotilinopathy. In mutant myotilin-expressing muscle fibers, myotilin aggregates and is costained with polyubiquitin, and Z-disk–associated proteins and myofibrillar disorganization were commonly seen. In addition, the expressed S60C mutant myotilin protein displayed marked detergent insolubility in electroporated mouse muscle, similar to that observed in human MFM muscle with the same mutation. Thus, *in vivo* electroporation can be a useful method for evaluating the pathogenicity of mutations identified in MFM. *(Am J Pathol 2012, 180: 1570–1580; DOI: 10.1016/j.ajpath.2011.12.040)*

Myofibrillar myopathy (MFM) is a group of neuromuscular diseases with common morphological features such as disorganized myofibrillar alignment and accumulation of Z-disk–associated proteins.[1] Mutations in genes encoding Z-disk–associated proteins are known to cause MFM. Disease-associated mutations have been identified in six genes, including myotilin, desmin, αB-crystallin, ZASP, filamin C, and BAG3.[2,3] Elucidation of their pathogenicity, however, is sometimes difficult.

Myotilin (myofibrillar protein with titin-like immunoglobulin domains) is a 57-kDa protein with 10 exons encoded by the myotilin gene (*MYOT*) on chromosome 5q31. Myotilin consists of a unique serine-rich domain at the N-terminus and two Ig-like domains at the C-terminus.[4–7] Myotilin is highly expressed in skeletal and cardiac muscle, and localizes to the Z-disk,[4] which plays important roles in sarcomere assembly, actin filament stabilization, and muscle force transmission.[8,9] Myotilin interacts with several Z-disk–associated proteins, including α-actinin,[4] filamin C,[10,11] FATZ,[11] ZASP,[12] and MuRF ubiquitin ligase.[13] Myotilin also interacts with actin monomers and filaments through its Ig-like domains, which also mediate homodimerization.[14] Previous studies have shown that myotilin can bundle actin filaments *in vitro*, acting alone or in collaboration with α-actinin and filamin C.[4,14,15] Thus, myotilin is thought to play a role in anchoring and stabilizing actin filaments at the Z-disk, and is involved in the organization and maintenance of Z-disk integrity.[12] Missense mutations in *MYOT* have been associated with MFM,[16–18] limb girdle muscular dystrophy type 1A,[17,19,20] and distal myopathy.[21,22] We have previously identified a mutation p.Arg405Lys (R405K) in exon 9 in the second Ig-like domain of myotilin. The R405K mutant myotilin exhibited defective homodimerization and decreased interaction with α-actinin in a yeast 2-hybrid (Y2H) system.[23] All of the other previously reported *MYOT* mutations are located in exon 2 [14,16–18,24], with p.Ser60Cys (S60C) being one of the most common mutations. The pathogenic effects of *MYOT* mutations and

Supported by a Grant-in-Aid for Scientific Research from the Japan Society for the Promotion of Science; a Comprehensive Research on Disability Health and Welfare (20B-12, 20B-13) award from the Ministry of Health, Labor and Welfare; a Research on Intractable Diseases award from the Ministry of Health, Labor and Welfare; an Intramural Research Grant (23-4, 23-5, 23-6) for Neurological and Psychiatric Disorders, National Center of Neurology and Psychiatry; and a grant from the Japan Foundation for Neuroscience and Mental Health.

Accepted for publication December 29, 2011.

Supplemental material for this article can be found at *http://ajp.amjpathol.org* or at doi: 10.1016/j.ajpath.2011.12.040.

Address reprint requests to Yukiko K. Hayashi, M.D, Ph.D., Department of Neuromuscular Research, National Institute of Neuroscience, National Center of Neurology and Psychiatry, 4-1-1 Ogawahigashicho, Kodaira, Tokyo, 187-8502, Japan. E-mail: hayasi_y@ncnp.go.jp.

the disease mechanism involved remain poorly understood.

Model animals, such as transgenic mice, have contributed to understanding of the critical pathogenic events in MFM.[25–27] Some MFMs, including myotilinopathies, are late-onset and slowly progressive diseases.[1,3] To reproduce clinical and pathological features in model animals for such late-onset mild myopathy is both labor intensive and time consuming. Among the 10 missense mutations identified to date in patients with myotilinopathy,[14,16–18,23,24] only the Thr57Ile (T57I) mutation reproduces the pathological changes in transgenic mice after 12 months of age.[28] To screen for candidate mutations in MFM, a new method is required for demonstrating the pathogenicity of mutations. In the present study, we expressed mutant myotilin in mouse muscle by *in vivo* electroporation and were able to easily reproduce pathological changes similar to those observed in skeletal muscle from patients with *MYOT* mutations.

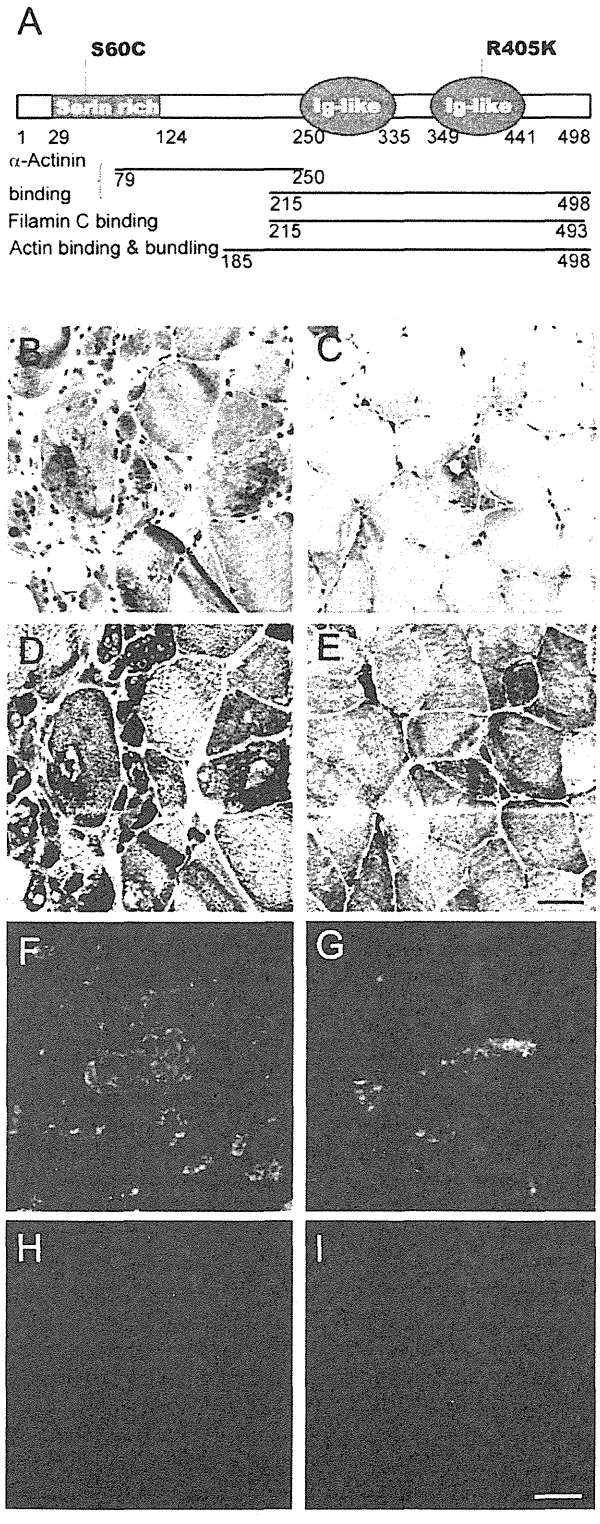

Materials and Methods

Clinical Materials

All clinical materials used in this study were obtained for diagnostic purposes with written informed consent. The studies were approved by the Ethical Committee of the National Center of Neurology and Psychiatry.

Genetic Analysis

Genomic DNA was isolated from peripheral lymphocytes or muscle specimens of patients, using standard techniques. Sequencing and mutation analysis of *MYOT* were performed as described previously.[23]

Plasmid Construction

We cloned full-length human myotilin cDNA and generated mutant myotilin (mMYOT) by site-directed mutagenesis, as described previously.[23] A C→G substitution at nucleotide position 179 and a G→A substitution at nucleotide 1214 were introduced to obtain p.S60C and p.R405K, respectively. A schematic of the location of these mutations in the structure of the myotilin protein is given in Figure 1A. For expression in mammalian cells, cDNAs of wild-type myotilin (wtMYOT) or mMYOT (S60C or R405K) were subcloned into pCMV-Myc vector (Ta-

Figure 1. Myotilin mutations and histopathological findings in myotilinopathy patients. **A:** Myotilin structure and disease-related mutations. p.Ser60Cys (S60C) is located in the serine-rich domain and p.Arg405Lys (R405K) is located in the second immunoglobulin (Ig)-like domain of myotilin. **B–I:** Pathological changes in muscles from patient 1 with *MYOT*S60C (**B**, **D**, **F**, and **H**) and from patient 2 with *MYOT*R405K (**C**, **E**, **G**, and **I**). **B:** Modified Gömöri trichrome (mGT) staining of biopsied skeletal muscle from patient 1 revealed markedly degenerated fibers with many spheroid protein inclusions (**arrows**). Some fibers had rimmed vacuoles (**arrowhead**). **C:** mGT staining of biopsied skeletal muscle from patient 2 revealed scattered fibers with rimmed vacuoles (**arrowhead**). **D:** NADH tetrazolium reductase (NADH-TR) staining of the serial section shown in **B** revealed markedly disorganized intermyofibrillar networks (**arrows**). **E:** NADH-TR staining of the serial section shown in **C** revealed disorganized intermyofibrillar networks (**arrow**). **F–I:** Coimmunostaining of muscles from patients using anti-myotilin (green) and anti-polyubiquitin (red) antibodies. **F:** Large accumulations of myotilin were observed in many fibers in patient 1. **G:** Small accumulations of myotilin were seen in some fibers in patient 2. Myotilin aggregates were positive for polyubiquitin in both patient 1 (**H**) and patient 2 (**I**). Scale bars: 50 μm (**B–E**); 20 μm (**F–I**).

kara Bio, Shiga, Japan). All constructs were verified by sequencing. Primer sequences are available on request.

Cell Culture, Transfection, and Immunocytochemical Analysis

C2C12 murine myoblast cells (American Type Culture Collection, Manassas, VA) were cultured in Dulbecco's modified Eagle's medium (Sigma-Aldrich, St. Louis, MO) supplemented with 10% fetal bovine serum (Invitrogen, Carlsbad, CA) at 37°C in a humidified atmosphere of 5% carbon dioxide. The cells were transiently transfected using FuGENE HD transfection reagent (Roche Diagnostics, Indianapolis, IN), according to the manufacturer's instructions. Forty-eight hours after transfection, the cells were fixed in 4% paraformaldehyde, permeabilized with 0.5% Triton-X 100, and costained with anti-Myc antibody (Sigma-Aldrich) and rhodamine-labeled phalloidin (Wako Pure Chemical Industries, Osaka, Japan) to detect transfected myotilin and actin filaments, respectively, according to standard protocol.[29]

In Vivo *Electroporation*

ICR mice were purchased from CLEA Japan (Fuji, Shizuoka, Japan). Animals were handled in accordance with the guidelines established by the Ethical Review Committee on the Care and Use of Rodents in the National Institute of Neuroscience, National Center of Neurology and Psychiatry. All mouse experiments were approved by the Committee. Five-week-old male ICR mice were anesthetized with diethyl ether, and the tibialis anterior (TA) muscles of mice were injected with 80 μg of purified Myc-tagged myotilin plasmid DNA. wtMYOT was injected to one side of TA muscle and mMYOT (S60C or R405K) was injected to the other side of TA muscle. *In vivo* transfection was performed using a square-wave electroporator (CUY-21SC; Nepa Gene, Ichikawa, Japan). A pair of electrode needles was inserted into the muscle to a depth of 3 mm to encompass the DNA injection sites. Each injected site was administered with three consecutive 50 ms-long pulses at the required voltage (50 to 90 V) to yield a current of 150 mA. After a 1-second interval, three consecutive pulses of the opposite polarity were administered. At 7 or 14 days after electroporation, mice were sacrificed by cervical dislocation, and TA muscles were isolated.

Histochemical and Immunohistochemical Analyses

Biopsied human muscles or electroporated mouse TA muscles were frozen in isopentane cooled in liquid nitrogen. Serial 10-μm cryosections were stained with modified Gömöri trichrome (mGT) and NADH-tetrazolium reductase (NADH-TR) and were subjected to a battery of histochemical methods. Immunohistochemistry was performed on serial 6-μm cryosections, as described previously.[29]

Antibodies

The primary antibodies used in this study were as follows: actin (Kantoukagaku, Tokyo, Japan), α-actinin (Sigma-Aldrich), BAG3 (Abcam, Tokyo, Japan), αB-crystallin (StressGen Biotechnologies, Victoria, BC, Canada), desmin (PROGEN Biotechnik, Heidelberg, Germany), filamin C (kindly provided by A.H. Beggs),[30] c-Myc (Sigma-Aldrich), c-Myc (PROGEN Biotechnik), myotilin (Proteintech Group, Chicago, IL), polyubiquitinated protein (Biomol International-Enzo Life Sciences, Plymouth Meeting, PA), GAPDH (Advanced ImmunoChemical, Long Beach, CA), and horseradish peroxidase-labeled anti-c-Myc antibody (Santa Cruz Biotechnology, Santa Cruz, CA).

Evaluation of Aggregates

Histochemical and immunohistochemical analyses were performed on cryosections of electroporated muscles sectioned at 500-μm intervals. The section containing the highest number of Myc-positive fibers (>100 fibers) was used. Myc-positive granules >1 μm in diameter were defined as aggregates. The Myc-positive fibers containing Myc-positive aggregates were counted among all Myc-positive fibers. Five mice each from the wtMYOT-, mMYOT S60C-, and mMYOT R405K-expressing groups were examined. To compare the number and size of Myc-positive aggregates per fiber, we measured the number and area of Myc-positive aggregates in 30 myofibers from each specimen using ImageJ software version 1.43 (NIH, Bethesda, MD). The results are presented as bar graphs (±SD) and histograms. Fifteen serial sections were immunoblotted to measure the amounts of electroporated Myc-tagged myotilin protein.

Electron Microscopy

For electron microscopy, cryosections (25 μm thick) of biopsied muscle with the S60C mutation (patient 1) were fixed with 2% glutaraldehyde in 100 mmol/L cacodylate buffer for 15 minutes on ice. After a shaking with a mixture of 4% osmium tetroxide, 1.5% lanthanum nitrate, and 200 mmol/L s-collidine for 1 to 2 hours, samples were embedded in epoxy resin. TA muscles of 5-week-old ICR mice were coelectroporated with pEGFP-C1 plasmid (Clontech, Tokyo, Japan), which encodes enhanced green fluorescent protein (EGFP), and with either Myc-wtMYOT or Myc-mMYOT (S60C or R405K) plasmid (40 μg each). As a control, pEGFP-C1 plasmid was electroporated alone. TA muscles were isolated 7 and 14 days after electroporation. EGFP-positive regions were trimmed under a fluorescence microscope and fixed with 2% glutaraldehyde in 100 mmol/L cacodylate buffer for 3 hours. After a shaking with a mixture of 4% osmium tetroxide, 1.5% lanthanum nitrate, and 200 mmol/L s-collidine for 2 to 3 hours, samples were embedded in epoxy resin. Semithin sections (1 μm thick) were stained with Toluidine Blue. Ultrathin sections (100 nm thick) were stained with uranyl acetate and lead citrate, and were analyzed at 120 kV using a Tecnai Spirit transmission electron microscope (FEI, Hillsboro, OR).

Solubility and Immunoblot Assay

To examine solubility of mutant myotilin, we used frozen biopsied muscles from human control subjects and from the two myotilinopathy patients, as well as TA muscles of six mice each from the wtMYOT-, mMYOT S60C-, and mMYOT R405K-expressing groups, at 14 days after electroporation. The 1.25-mm^3 specimens of muscle were lysed and homogenized in 150 μL of radioimmunoprecipitation assay buffer containing 50 mmol/L Tris-HCl (pH 7.5), 150 mmol/L NaCl, 1 mmol/L EDTA (pH 8.0), 1% Nonidet P-40, 0.5% sodium deoxycholate, 0.1% SDS, and Roche complete protease inhibitor cocktail (Roche Diagnostics). The lysates were incubated at 4°C for 20 minutes with gentle rotation, and then centrifuged at 15,000 × *g* at 4°C for 20 minutes. The supernatants and precipitates were collected, and the protein concentrations of the supernatants were determined using a protein assay kit (Bio-Rad Laboratories, Hercules, CA). Immunoblotting of the supernatant (detergent-soluble) and precipitate (detergent-insoluble) fractions was performed, as described previously.[23] Glyceraldehyde 3-phosphate dehydrogenase (GAPDH) was used as an internal standard. Immunoreactive complexes on the membranes were detected using enhanced chemiluminescence ECL Plus detection reagent (GE Healthcare, Chalfont St Giles, UK). Insolubility index was calculated as the ratio of the quantity of insoluble protein to the total quantity of proteins (the sum of soluble and insoluble proteins).

Immunoprecipitation

The 5-mm^3 specimens of frozen electroporated mouse muscles isolated at 14 days after electroporation were lysed and homogenized in 0.6 mL of radioimmunoprecipitation assay buffer. The lysates were incubated at 4°C for 20 minutes with gentle rotation, and then centrifuged at 15,000 × *g* at 4°C for 20 minutes. The supernatants were collected, and their protein concentrations were adjusted using a protein assay kit (Bio-Rad Laboratories). Immunoprecipitation was performed as described previously,[23] with agarose-conjugated anti-Myc antibody (Santa Cruz Biotechnology).

Statistical Analysis

Differences between wtMYOT-, mMYOT S60C-, and mMYOT R405K-expressing mice were analyzed with GraphPad Prism version 5 (GraphPad Software, La Jolla, CA). Comparisons among groups were performed by one-way analysis of variance with post hoc Tukey's analysis. Data are expressed as means ± SD.

Results

Mutation Screening and Histochemical Analyses of Muscles from Patients

We performed *MYOT* mutation screening in MFM patients and identified two patients with mutations. Patient 1, harboring a *MYOT* c.179C→G (p.S60C) mutation in exon 2, was a 63-year-old woman with a 6-year-long history of slowly progressive limb muscle weakness. Her mother (deceased) had had muscle weakness. The patient had difficulty in climbing stairs without support, and could not walk for long distances. Her serum creatine kinase level was elevated to 734 IU/L (reference, <200 IU/L). A biopsied specimen from the rectus femoris muscle showed marked variation in fiber size, with some necrotic fibers. Clusters of degenerated fibers with abnormal cytoplasmic inclusions were observed; some fibers with rimmed vacuoles were also seen (Figure 1B). Intermyofibrillar networks were markedly disorganized (Figure 1D). Under electron microscopy, electron-dense materials and cytoplasmic amorphous inclusions of various sizes were seen in some fibers (see Supplemental Figure S1 at *http://ajp.amjpathol.org*). Patient 2 was a 57-year-old woman harboring a *MYOT* c.1214G→A (p.R405K) mutation in exon 9. Detailed clinical symptoms have been described previously.[23] In brief, this patient had a 16-year-long history of slowly progressive proximal limb muscle weakness. Her serum creatine kinase level was mildly elevated (385 IU/l). A specimen from the vastus lateralis muscle showed marked variation in fiber size, scattered fibers with internal nuclei, and small angular fibers. Some fibers with rimmed vacuoles were seen (Figure 1C), and intermyofibrillar networks were disorganized (Figure 1E). Immunohistochemical analysis of muscle specimens from both patients revealed scattered fibers with strong immunoreactive accumulations of myotilin (Figure 1, F and G), which costained with polyubiquitin (Figure 1, H and I), α-B crystallin, BAG3, actin, desmin, and filamin C (see Supplemental Figure S2 at *http://ajp.amjpathol.org*).

Mutant Myotilin Does Not Aggregate in Cultured Cells

To examine the aggregation of mutant myotilins in cultured cells, C2C12 murine myoblasts were transfected with Myc-tagged wtMYOT (Myc-wtMYOT) or Myc-tagged mMYOT (Myc-mMYOT S60C or R405K). After 48 hours, immunostaining with anti-Myc antibody and rhodamine-labeled phalloidin revealed that the expressed Myc-wtMYOT, Myc-mMYOT S60C, and Myc-mMYOT R405K did not form abnormal protein aggregations, and they localized at actin stress fibers (Figure 2). Expression of mMYOT did not affect differentiation of C2C12 cells (data not shown).

Accumulation of Myotilin after Electroporation

To investigate the roles of mutant myotilin, we performed *in vivo* electroporation to express Myc-wtMYOT or Myc-mMYOT (S60C or R405K) in mouse TA muscles. At 7 and 14 days after electroporation, Myc-positive granules with diameters >1 μm were observed in Myc-tagged myotilin-expressing myofibers (Figure 3A). Compared with wtMYOT-expressing myofibers, mMYOT-expressing myofi-

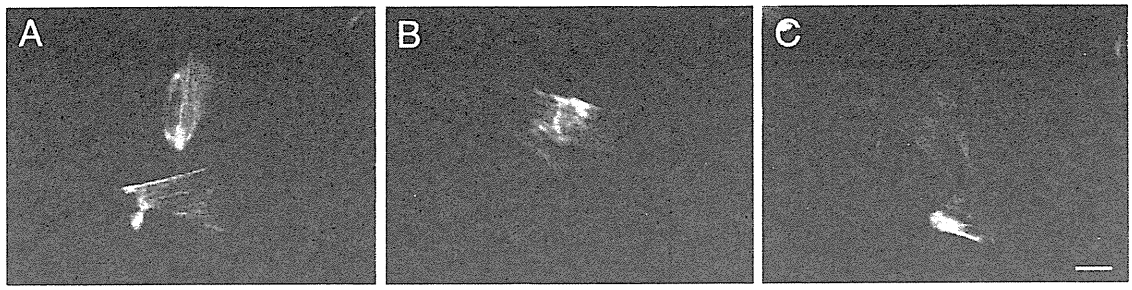

Figure 2. Expression of mutant myotilin in cultured cells. Immunofluorescence staining of transfected Myc-wtMYOT (**A**), Myc-mMYOT S60C (**B**), and Myc-mMYOT R405K (**C**) in C2C12 murine myoblasts. Merged images of Myc-tagged myotilin-expressing cells (green) costained for actin stress fibers (red), and nuclear staining with DAPI (blue). C2C12 myoblasts expressing mMYOT S60C (**B**) or R405K (**C**) did not exhibit protein aggregates, and the mutant myotilin colocalized with actin stress fibers similar to wtMYOT (**A**). Scale bar = 20 μm.

bers contained more granular aggregates that were larger in size. At 7 days after electroporation, Myc-positive aggregates of wtMYOT, mMYOT S60C, and mMYOT R405K were observed in 14 ± 5%, 44 ± 7%, and 21 ± 4% of muscle fibers, respectively (Figure 3B). At 14 days after electroporation, the number of the fibers with aggregates increased to 22 ± 4% in wtMYOT, 50 ± 2% in mMYOT S60C, and 37 ± 3% in mMYOT R405K (Figure 3C). The number and size of Myc-positive aggregates in 30 randomly selected Myc-positive muscle fibers were much higher in mMYOT S60C and slightly higher in mMYOT R405K at 14 days after electroporation than at 7 days (see Supplemental Figure S3 at *http://ajp.amjpathol.org*). These data indicate that the expressed mutant myotilins, and mMYOT S60C in particular, are prone to aggregate in skeletal muscles. The amounts of expressed Myc-tagged myotilin proteins were approximately equal, as measured by immunoblotting (Figure 3D).

Myofibril Disorganization and Z-Disk Streaming in Muscles Expressing Mutant Myotilins

To investigate the ultrastructural characteristics of mutant myotilin-electroporated muscles, we performed electron microscopy at 7 and 14 days after electroporation. In Toluidine Blue-stained longitudinal semithin sections, partial disorganization of the Z-disk was observed in both mMYOT S60C-expressing and mMYOT R405K-expressing TA muscles, but not in control or wtMYOT electroporated muscles (data not shown). Electron microscopy also revealed myofibril disorganization with disrupted Z-disk, such as Z-disk streaming and broadening, in mMYOT-expressing muscles (Figure 4, A and D). Variable-sized (1 to 8 μm in diameter) electron-dense material, with electron densities similar to that of the Z-disk, were also seen in mMYOT-expressing mouse muscles (Figure 4, B and E). The inclusions were occasionally associated with autophagic vacuoles (Figure 4, C and F). These ultrastructural findings were commonly observed in both mMYOT S60C- and mMYOT R405K-expressing mouse muscles.

Mutant Myotilin Aggregates Colocalize with Polyubiquitin and Other Z-Disk–Associated Proteins

To compare the protein accumulations in human and mouse muscles, we performed immunohistochemical analysis. At 14 days after electroporation, some cytoplasmic inclusions were observed in mGT-stained sections of mMYOT-expressing muscles (Figure 5, A and B). Immunostaining of serial sections revealed that the inclusions were immunopositive for the Myc tag (Figure 5, A and B). The aggregates of Myc-mMYOT (S60C and R405K) strongly colocalized with polyubiquitin and αB-crystallin. Accumulations of other Z-disk–associated proteins were also observed, including BAG3, actin, desmin, and filamin C (Figure 5). These findings are similar to the observations made in the patients' muscles (Figure 1, F–I; see also Supplemental Figure S2 at *http://ajp.amjpathol.org*). In the electroporated muscles, Myc-wtMYOT aggregates also colocalized with Z-disk–associated proteins, including αB-crystallin, BAG3, actin, desmin, and filamin C (data not shown), whereas only few wtMYOT aggregates were immunopositive for polyubiquitin (Figure 6A).

Mutant Myotilin Proteins Display Marked Detergent Insolubility with Polyubiquitinated Proteins

In the muscle specimens of the two myotilinopathy patients, myotilin aggregates exhibited positive staining for polyubiquitin (Figure 1; see also Supplemental Figure S3 at *http://ajp.amjpathol.org*). Similarly, in electroporated mouse muscles, mMYOT aggregates were positive for polyubiquitin, and polyubiquitin-positive aggregates were more prominently observed in mMYOT S60C-expressing muscles at 14 days after electroporation. On the other hand, only few aggregates of Myc-wtMYOT were positive for polyubiquitin (Figure 6A). This result suggests that mutant myotilin was ubiquitinated or that the expressed mutant myotilin induced the deposition of polyubiquitinated proteins in the muscles of patients and electroporated mice. To characterize these aggregates, we performed a solubility assay. The muscle

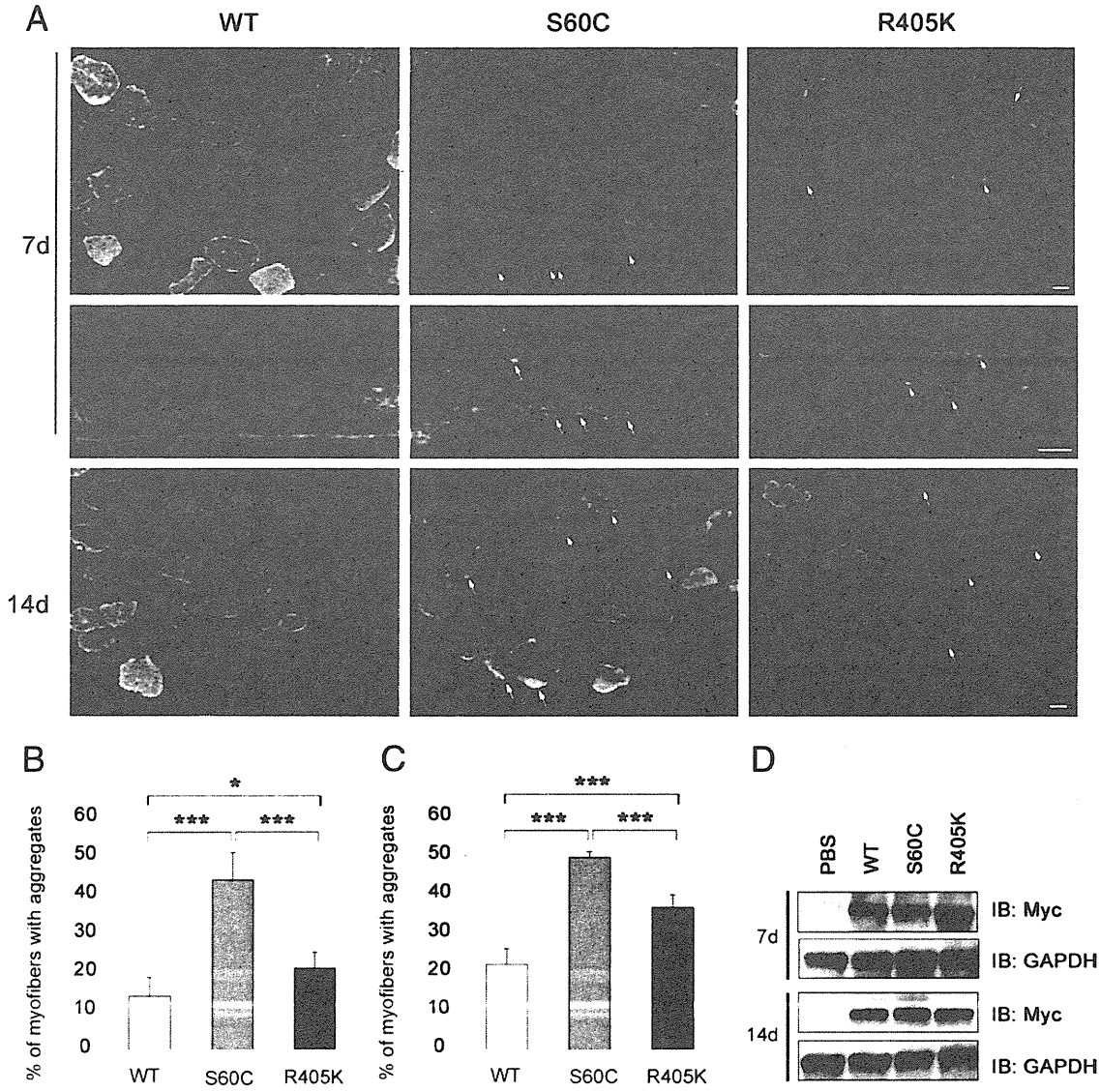

Figure 3. Enhanced aggregation of mutant myotilins in mouse skeletal muscle. **A:** Immunohistochemical staining of Myc-wtMYOT (WT)-electroporated or Myc-mMYOT (S60C or R405K)-electroporated mouse TA muscles. At 7 and 14 days after electroporation, S60C and R405K formed many Myc-positive granular aggregates (**arrows**) in myofibers, compared with WT. More prominent protein aggregates were observed in the S60C-electroporated muscle. At 14 days after electroporation, S60C-expressing myofibers exhibited larger aggregates. Scale bars: 20 μm. **B** and **C:** The percentage of myofibers with Myc-positive aggregates in the electroporated fibers of the WT, S60C, and R405K expression groups (n = 5 mice per group). $^{*}P < 0.05$; $^{***}P < 0.001$. **D:** Immunoblotting analysis of transfected Myc-tagged myotilin in 15 serial sections taken after the sections used for immunohistochemistry. GAPDH was used as a loading control.

specimen with the S60C mutation (patient 1) exhibited increased amounts of myotilin in the detergent-insoluble fraction, compared with the control specimens (Figure 6, B and D). Increasing amounts of polyubiquitinated proteins and αB-crystallin were also detected in the insoluble fraction. On the other hand, the solubilities of myotilin and other proteins, including polyubiquitin, in the muscle specimen with the R405K mutation (patient 2) were similar to those of controls (Figure 6B). Consistently, in the mouse muscles isolated at 14 days after electroporation, markedly increasing amounts of insoluble mMYOT S60C were observed (Figure 6C). In the PBS-injected control muscle, insolubility of endogenous myotilin was 31 ± 12%, whereas in the wtMYOT-, mMYOT S60C-, and mMYOT R405K-injected muscles, the Myc-tagged myotilin amounts in the insoluble fraction were 34 ± 10%, 69 ± 5%, and 48 ± 9%, respectively (Figure 6E). Insolubility of Myc-wtMYOT was similar to that of endogenous myotilin, but mMYOT, and S60C in particular, exhibited higher insolubility (Figure 6E).

These results are consistent with the number of intracellular aggregates observed after electroporation. The amount of polyubiquitinated proteins was markedly increased in the insoluble fraction of mMYOT S60C-electroporated muscles, similar to that of the muscle with the S60C mutation (patient 1) (Figure 6, B and C). A slight increase in the amount of detergent-insoluble polyubiquitinated proteins was observed in mMYOT R405K-electroporated muscles (Figure 6C). The amounts of other

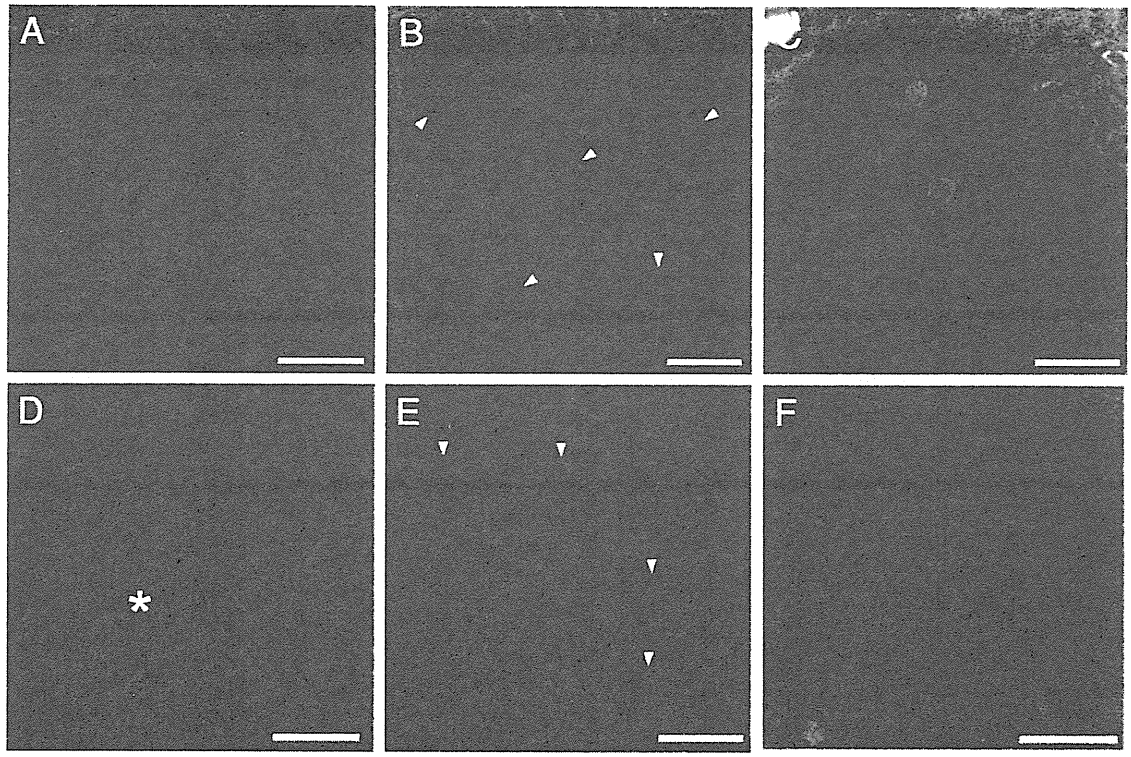

Figure 4. Electron microscopy of muscles expressing mutant myotilin. mMYOT S60C (**A–C**); mMYOT R405K (**D–F**). **A** and **D:** mMYOT-transfected muscle fibers exhibited myofibril disorganization with disrupted Z-disk; note broadening of Z-disks (**A**, **brackets**) and Z-disk streaming (**D**, **asterisk**). **B** and **E:** Variable-sized (1 to 8 μm in diameter) electron-dense inclusions (**arrowheads**) were seen in mMYOT-expressing muscles. **C** and **F:** Inclusions were occasionally associated with autophagic vacuoles (AV). **B** and **C:** Seven days after electroporation. **A** and **D–F:** Fourteen days after electroporation. Scale bars: 3.0 μm (**B** and **E**); 2.0 μm (**C**); 1.7 μm (**A** and **D**); 1.4 μm (**F**).

Z-disk–associated proteins, including αB-crystallin, in the insoluble fraction did not exhibit an increase, even in mMYOT S60C-electroporated muscles (Figure 6C; see also Supplemental Figure S4, A and B, at *http://ajp.amjpathol.org*). We also performed an immunoprecipitation assay to examine whether myotilin was polyubiquitinated. Myc-tagged myotilin proteins were immunoprecipitated from the detergent-soluble fraction of the mouse muscles isolated at 14 days after electroporation. Polyubiquitin immunoreactivity was not detected in the immunoprecipitated proteins (see Supplemental Figure S4C at *http://ajp.amjpathol.org*), indicating that neither the wt-MYOT nor the mMYOT proteins in the soluble fraction were polyubiquitinated.

Discussion

Patients with MFM, including myotilinopathy, exhibit variable clinical features. Some patients exhibit progressive weakness in proximal muscles, whereas others exhibit distal dominant muscle involvement. Cardiomyopathy, peripheral neuropathy, and respiratory insufficiency may be observed.[2] The diagnosis of MFM is generically based on characteristic pathological findings in biopsied muscles, namely, myofibrillar degradation and protein aggregation.[1] Histochemically, the most remarkable pathological changes were observed with mGT staining (Figure 1). Abnormal protein aggregates were observed, including amorphous, granular, or hyaline deposits of various sizes, shapes, and colors (dark blue, blue red, or dark green). The presence of rimmed and nonrimmed vacuoles was also a characteristic observation. Furthermore, NADH-TR staining revealed intermyofibrillar network disorganization. Attenuation or absence of NADH-TR activity in focal areas of myofibers is also observed in MFM.[1,31]

Here, we have presented findings for myotilinopathy patients with similar clinical features but different pathological changes. Fibers with cytoplasmic inclusions and disorganized myofibrils were prominent in the patient with S60C mutation, and these inclusions were strongly immunoreactive for myotilin (Figure 1).

Although transfected cultured cells did not show aggregations, our *in vivo* expression studies in mice were able to reproduce the pathological changes observed in myotilinopathy patients. Mutant myotilin caused enhanced protein aggregation in TA muscles within 1 to 2 weeks (Figure 3). The dark blue or dark green inclusions stained by mGT in mutant-expressing fibers (Figure 4) were similar to those observed in the myotilinopathy patients. Furthermore, mMYOT S60C-expressing myofibers exhibited a greater number of aggregates, which is consistent with the pathology of the patient with that mutation (patient 1). Of note, the size of mMYOT S60C aggregates markedly increased over time, suggesting that mutant myotilin may be resistant to protein degra-

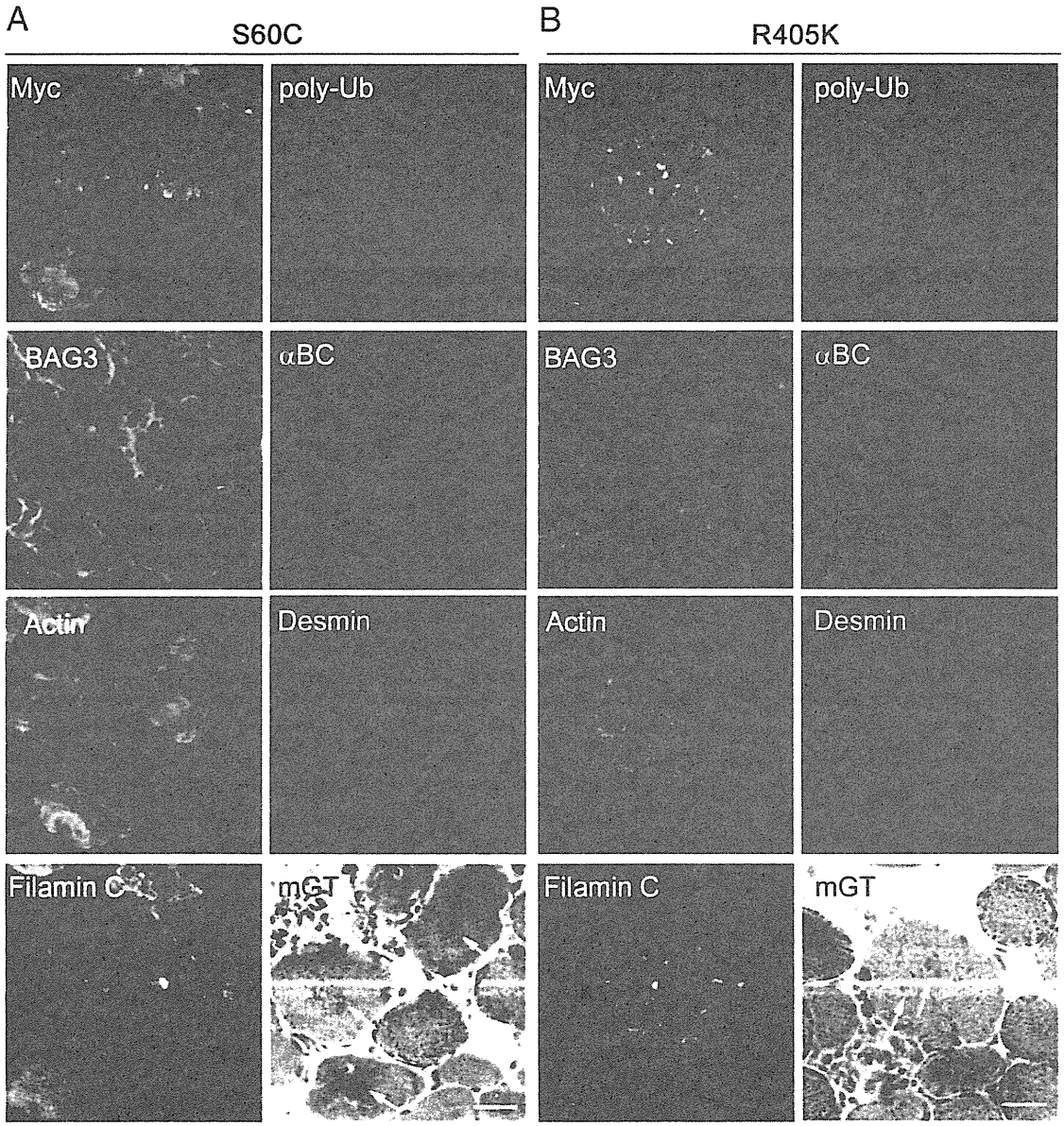

Figure 5. Mutant myotilin aggregates colocalize with polyubiquitin and other Z-disk–associated proteins in electroporated mouse muscle. mGT and immunohistochemical staining of mouse muscle expressing Myc-mMYOT S60C (**A**) or mMYOT R405K (**B**) at 14 days after electroporation. On mGT-stained sections of mMYOT-expressing muscles, cytoplasmic inclusions (**arrows**) were seen. The inclusions were immunopositive for the Myc tag in serial sections. The Myc-positive aggregates of S60C and R405K strongly colocalized with polyubiquitin (poly-Ub) and αB-crystallin (αBC). The aggregates were also immunopositive for BAG3, actin, desmin, and filamin C. Scale bars: 20 μm (**A** and **B**).

dation, as described previously for MFM-associated mutant desmin.[32,33]

Focal disorganization of myofibrils, Z-disk streaming, and accumulation of electron-dense material near the Z-disk are characteristic electron microscopic findings in the muscles of MFM patients.[17,34,35] In the myotilinopathy patient, Z-disk streaming, numerous autophagic vacuoles[17] and cytoplasmic amorphous inclusions were observed (see Supplemental Figure S2 at *http://ajp.amjpathol.org*). In the present study, expression of mMYOT by electroporation elicited myofibril disorganization and accumulation of electron-dense material, which are ultrastructural hallmarks of MFM (Figure 5). Autophagic vacuoles associated with inclusions were also observed in electroporated muscles. Disorganization of myofibrils starting from the Z-disk and material appearing to originate from the Z-disk are commonly observed in MFM patients,[34,35] and these features were also observed in the mMYOT-electroporated muscles. These morphological findings imply that the presence of mutant myotilin can induce characteristic pathological features by affecting Z-disk structure.

Ectopic accumulations of multiple proteins, including Z-disk–associated proteins, are typical pathological features of MFM.[36,37] This study and previous reports[23,38] showed that myotilin-positive protein aggregates colocal-

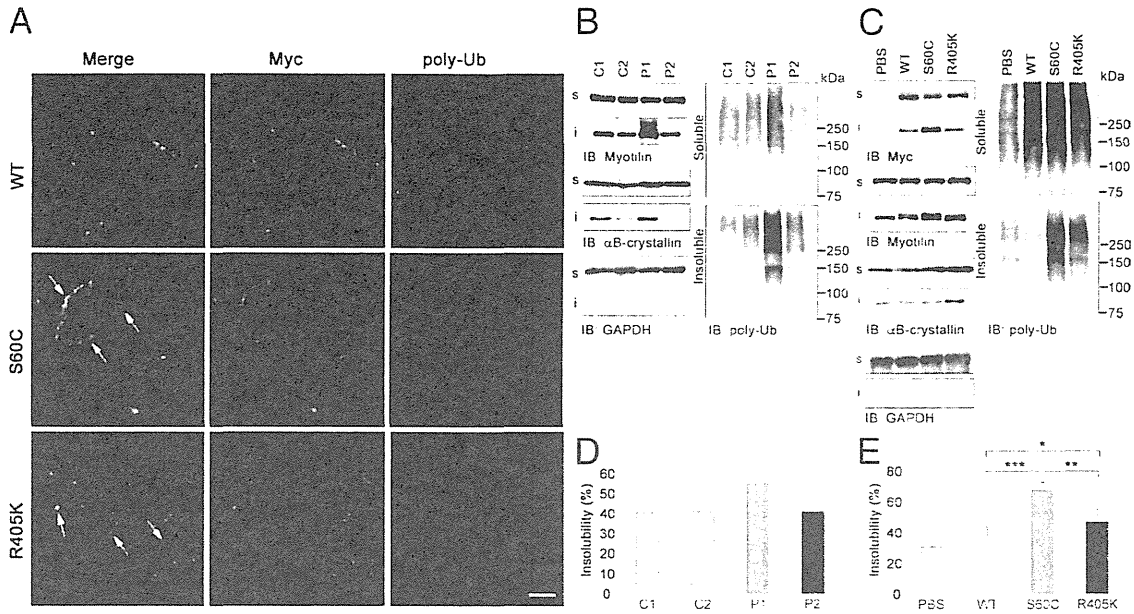

Figure 6. Mutant myotilin displays marked detergent insolubility, along with polyubiquitinated proteins. **A:** At 14 days after electroporation of Myc-wtMYOT (WT) or Myc-mMYOT (S60C or R405K), Myc-mMYOT aggregates, particularly those of S60C, colocalized with polyubiquitin (poly-Ub) (**arrows**). The WT aggregates rarely costained with polyubiquitin. **B–E** Solubilities of myotilin, polyubiquitinated proteins, and other sarcomeric proteins in muscles from myotilinopathy patients (**B** and **D**) and from electroporated mice (**C** and **E**). GAPDH was used as a loading control. **B:** Immunoblotting of detergent-soluble and detergent-insoluble fractions of muscles from control subjects (C1 and C2) or myotilinopathy patients [P1 (patient 1) and P2 (patient 2)]. In the muscles from P1 with S60C, markedly increasing amounts of myotilin, polyubiquitinated proteins, and αB-crystallin were detected in the insoluble fraction, compared with muscles from control subjects. **D:** Quantification of myotilin insolubilities revealed highest insolubility in P1. **C:** Immunoblotting of detergent-soluble and detergent-insoluble fractions of WT, S60C, or R405K-expressing muscles at 14 days after electroporation. Increasing amounts of insoluble Myc-tagged myotilin proteins and polyubiquitinated proteins were observed in mMYOT-electroporated muscles, compared with WT. Particularly in S60C-electroporated muscles, the amounts of insoluble proteins were notably increased. **E:** Quantification of the insolubilities of electroporated Myc-tagged myotilin in the WT, S60C, and R405K expression groups ($n = 6$ mice per group). Insolubility of endogenous myotilin was measured using PBS-treated mouse muscles. Compared with WT, insolubilities of electroporated Myc-tagged myotilin were significantly increased in S60C and R405K. $^{*}P < 0.05$; $^{**}P < 0.01$; $^{***}P < 0.001$. Scale bar = 20 μm.

ize with ubiquitin and Z-disk–associated proteins (ie, αB-crystallin, BAG3, actin, desmin, and filamin C) in the muscles of myotilinopathy patients (Figure 1; see also Supplemental Figure S2 at *http://ajp.amjpathol.org*). It has been reported that the myotilin T57I transgenic mice develop progressive myofibrillar changes, including Z-disk streaming and accumulation of mutant myotilin with ubiquitin and Z-disk–associated proteins, similar to those observed in myotilinopathy patients.[28] Expression of mMYOT elicited similar cytoplasmic aggregations in mouse skeletal muscle, and within 2 weeks the aggregates colocalized with polyubiquitin and other Z-disk–associated proteins. Our results indicate that mutant myotilin is able to nucleate aggregations of Z-disk–associated proteins in skeletal muscle.

MFM is a proteinopathy (ie, a protein accumulation disease). In these diseases, protein aggregates are operationally defined by poor solubility in aqueous or detergent solvents.[39,40] Such insoluble protein aggregations are characteristic of many neurodegenerative diseases.[41] In the present study, we discovered that the mutant myotilin S60C protein, along with polyubiquitinated proteins, exhibited marked detergent insolubility in muscles from both the patient and electroporated mice. Mutant myotilin R405K protein showed increased, but lower, detergent insolubility in mice (Figure 6), which may be consistent with the observation that the muscle from the patient with the R405K mutation exhibited only mild protein aggregation (Figure 1). The different detergent insolubilities exhibited by the two *MYOT* mutations may closely correlate with the amounts of protein aggregation. Here, we confirmed the aggregation-prone property of mutant myotilin, which participates in the pathogenesis of myotilinopathy. Using an immunoprecipitation assay, we also showed that electroporated mMYOT was not ubiquitinated in the detergent-soluble fraction (see Supplemental Figure S4 at *http://ajp.amjpathol.org*). A previous study showed that transfected myotilin is degraded by the proteasome system in cultured cells.[42] Our present findings show that ubiquitinated mutant myotilin can form insoluble aggregates. It is also possible that aggregation of insoluble ubiquitinated proteins is induced by the expression of mutant myotilin.

Several causative genes have been identified for MFM; however, in previous studies no mutations were found in nearly half of the MFM patients.[2] To identify the unknown causative genes, easy methods are required for determining the pathogenicity of novel mutations. Some mutant proteins exhibit protein aggregation[43–45] or biological dysfunction, including protein-protein interaction *in vitro*.[23,46–48] However, we could not detect any protein aggregation in mMYOT-expressing cultured cells (Figure 2). The difficulty of *in vitro* investigation may be responsible for the inability to identify Z-disk–associated proteins or mature Z-disk structures. Indeed, myotilin is expressed in later differentiated C2C12 myotubes with

sarcomere-like structures.[49] This suggests that mutant myotilin requires mature Z-disk and/or other sarcomeric proteins to cause aggregations. In such cases, *in vivo* examination is important for evaluating the pathogenicity of mutations. Because *in vivo* electroporation can reproduce the pathological changes observed in MFM patients within a short time, it is a useful and powerful tool for evaluating the pathogenicity of mutations in MFM.

Acknowledgments

We thank Dr. Alan H. Beggs (Children's Hospital Boston, Harvard Medical School) for the kind gift of anti-filamin C antibody and Dr. Satomi Mitsuhashi (Children's Hospital Boston, Harvard Medical School) for technical assistance in electron microscopy analysis.

References

1. Selcen D: Myofibrillar myopathies. Neuromuscul Disord 2011, 21: 161–171
2. Selcen D, Engel AG: Myofibrillar myopathy. (Updated) In GeneReviews. Copyright University of Washington, Seattle. 1997–2012. Available at http://www.ncbi.nlm.nih.gov/books/NBK1499, last revised July 27, 2010
3. OlivÉ M, Odgerel Z, Martínez A, Poza JJ, Bragado FG, Zabalza RJ, Jericó I, Gonzalez-Mera L, Shatunov A, Lee HS, Armstrong J, Maravi E, Arroyo MR, Pascual-Calvet J, Navarro C, Paradas C, Huerta M, Marquez F, Rivas EG, Pou A, Ferrer I, Goldfarb LG: Clinical and myopathological evaluation of early- and late-onset subtypes of myofibrillar myopathy. Neuromuscul Disord 2011, 21:533–542
4. Salmikangas P, Mykkänen OM, Grönholm M, Heiska L, Kere J, Carpén O: Myotilin, a novel sarcomeric protein with two Ig-like domains, is encoded by a candidate gene for limb-girdle muscular dystrophy. Hum Mol Genet 1999, 8:1329–1336
5. Parast MM, Otey CA: Characterization of palladin, a novel protein localized to stress fibers and cell adhesions. J Cell Biol 2000, 150: 643–656
6. Mykkänen OM, Grönholm M, Rönty M, Lalowski M, Salmikangas P, Suila H, Carpén O: Characterization of human palladin, a microfilament-associated protein. Mol Biol Cell 2001, 12:3060–3073
7. Bang ML, Mudry RE, McElhinny AS, Trombitas K, Geach AJ, Yamasaki R, Sorimachi H, Granzier H, Gregorio CC, Labeit S: Myopalladin, a novel 145-kilodalton sarcomeric protein with multiple roles in Z-disc and I-band protein assemblies. J Cell Biol 2001, 153:413–427
8. Faulkner G, Lanfranchi G, Valle G: Telethonin and other new proteins of the Z-disc of skeletal muscle. IUBMB Life 2001, 51:275–282
9. Frank D, Kuhn C, Katus HA, Frey N: The sarcomeric Z-disc: a nodal point in signalling and disease. J Mol Med (Berl) 2006, 84:446–468
10. van der Ven PF, Wiesner S, Salmikangas P, Auerbach D, Himmel M, Kempa S, Hayess K, Pacholsky D, Taivainen A, Schröder R, Carpén O, Fürst DO: Indications for a novel muscular dystrophy pathway. gamma-Filamin, the muscle-specific filamin isoform, interacts with myotilin. J Cell Biol 2000, 151:235–248
11. Gontier Y, Taivainen A, Fontao L, Sonnenberg A, van der Flier A, Carpen O, Faulkner G, Borradori L: The Z-disc proteins myotilin and FATZ-1 interact with each other and are connected to the sarcolemma via muscle-specific filamins. J Cell Sci 2005, 118:3739–3749
12. von Nandelstadh P, Ismail M, Gardin C, Suila H, Zara I, Belgrano A, Valle G, Carpen O, Faulkner G: A class III PDZ binding motif in the myotilin and FATZ families binds enigma family proteins: a common link for Z-disc myopathies. Mol Cell Biol 2009, 29:822–834
13. Witt SH, Granzier H, Witt CC, Labeit S: MURF-1 and MURF-2 target a specific subset of myofibrillar proteins redundantly: towards understanding MURF-dependent muscle ubiquitination. J Mol Biol 2005, 350:713–722
14. Salmikangas P, van der Ven PF, Lalowski M, Taivainen A, Zhao F, Suila H, Schröder R, Lappalainen P, Fürst DO, Carpén O: Myotilin, the limb-girdle muscular dystrophy 1A (LGMD1A) protein, cross-links actin filaments and controls sarcomere assembly. Hum Mol Genet 2003, 12:189–203
15. von Nandelstadh P, Grönholm M, Moza M, Lamberg A, Savilahti H, Carpén O: Actin-organising properties of the muscular dystrophy protein myotilin. Exp Cell Res 2005, 310:131–139
16. Selcen D: Myofibrillar myopathies. Curr Opin Neurol 2008, 21:585–589
17. Olivé M, Goldfarb LG, Shatunov A, Fischer D, Ferrer I: Myotilinopathy: refining the clinical and myopathological phenotype. Brain 2005, 128:2315–2326
18. Foroud T, Pankratz N, Batchman AP, Pauciulo MW, Vidal R, Miravalle L, Goebel HH, Cushman LJ, Azzarelli B, Horak H, Farlow M, Nichols WC: A mutation in myotilin causes spheroid body myopathy. Neurology 2005, 65:1936–1940
19. Hauser MA, Conde CB, Kowaljow V, Zeppa G, Taratuto AL, Torian UM, Vance J, Pericak-Vance MA, Speer MC, Rosa AL: Myotilin mutation found in second pedigree with LGMD1A. Am J Hum Genet 2002, 71:1428–1432
20. Hauser MA, Horrigan SK, Salmikangas P, Torian UM, Viles KD, Dancel R, Tim RW, Taivainen A, Bartoloni L, Gilchrist JM, Stajich JM, Gaskell PC, Gilbert JR, Vance JM, Pericak-Vance MA, Carpen O, Westbrook CA, Speer MC: Myotilin is mutated in limb girdle muscular dystrophy 1A. Hum Mol Genet 2000, 9:2141–2147
21. Penisson-Besnier I, Talvinen K, Dumez C, Vihola A, Dubas F, Fardeau M, Hackman P, Carpen O, Udd B: Myotilinopathy in a family with late onset myopathy. Neuromuscul Disord 2006, 16:427–431
22. Berciano J, Gallardo E, Dominguez-Perles R, Garcia A, Garcia-Barredo R, Combarros O, Infante J, Illa I: Autosomal-dominant distal myopathy with a myotilin S55F mutation: sorting out the phenotype. J Neurol Neurosurg Psychiatry 2008, 79:205–208
23. Shalaby S, Mitsuhashi H, Matsuda C, Minami N, Noguchi S, Nonaka I, Nishino I, Hayashi YK: Defective myotilin homodimerization caused by a novel mutation in MYOT exon 9 in the first Japanese limb girdle muscular dystrophy 1A patient. J Neuropathol Exp Neurol 2009, 68:701–707
24. Reilich P, Krause S, Schramm N, Klutzny U, Bulst S, Zehetmayer B, Schneiderat P, Walter MC, Schoser B, Lochmüller H: A novel mutation in the myotilin gene (MYOT) causes a severe form of limb girdle muscular dystrophy 1A (LGMD1A). J Neurol 2011, 258:1437–1444
25. Mavroidis M, Panagopoulou P, Kostavasili I, Weisleder N, Capetanaki Y: A missense mutation in desmin tail domain linked to human dilated cardiomyopathy promotes cleavage of the head domain and abolishes its Z-disc localization. FASEB J 2008, 22:3318–3327
26. Wang X, Osinska H, Klevitsky R, Gerdes AM, Nieman M, Lorenz J, Hewett T, Robbins J: Expression of R120G-alphaB-crystallin causes aberrant desmin and alphaB-crystallin aggregation and cardiomyopathy in mice. Circ Res 2001, 89:84–91
27. Wang X, Osinska H, Dorn GW 2nd, Nieman M, Lorenz JN, Gerdes AM, Witt S, Kimball T, Gulick J, Robbins J: Mouse model of desmin-related cardiomyopathy. Circulation 2001, 103:2402–2407
28. Garvey SM, Miller SE, Claflin DR, Faulkner JA, Hauser MA: Transgenic mice expressing the myotilin T57I mutation unite the pathology associated with LGMD1A and MFM. Hum Mol Genet 2006, 15:2348–2362
29. Hayashi YK, Matsuda C, Ogawa M, Goto K, Tominaga K, Mitsuhashi S, Park YE, Nonaka I, Hino-Fukuyo N, Haginoya K, Sugano H, Nishino I: Human PTRF mutations cause secondary deficiency of caveolins resulting in muscular dystrophy with generalized lipodystrophy. J Clin Invest 2009, 119:2623–2633
30. Thompson TG, Chan YM, Hack AA, Brosius M, Rajala M, Lidov HG, McNally EM, Watkins S, Kunkel LM: Filamin 2 (FLN2): A muscle-specific sarcoglycan interacting protein. J Cell Biol 2000, 148:115–126
31. Schröder R, Schoser B: Myofibrillar myopathies: a clinical and myopathological guide. Brain Pathol 2009, 19:483–492
32. Liu J, Chen Q, Huang W, Horak KM, Zheng H, Mestril R, Wang X: Impairment of the ubiquitin-proteasome system in desminopathy mouse hearts. FASEB J 2006, 20:362–364
33. Liu J, Tang M, Mestril R, Wang X: Aberrant protein aggregation is essential for a mutant desmin to impair the proteolytic function of the ubiquitin-proteasome system in cardiomyocytes. J Mol Cell Cardiol 2006, 40:451–454
34. Selcen D, Ohno K, Engel AG: Myofibrillar myopathy: clinical, morphological and genetic studies in 63 patients. Brain 2004, 127:439–451

35. Claeys KG, Fardeau M, Schröder R, Suominen T, Tolksdorf K, Behin A, Dubourg O, Eymard B, Maisonobe T, Stojkovic T, Faulkner G, Richard P, Vicart P, Udd B, Voit T, Stoltenburg G: Electron microscopy in myofibrillar myopathies reveals clues to the mutated gene. Neuromuscul Disord 2008, 18:656–666
36. Claeys KG, van der Ven PF, Behin A, Stojkovic T, Eymard B, Dubourg O, Laforêt P, Faulkner G, Richard P, Vicart P, Romero NB, Stoltenburg G, Udd B, Fardeau M, Voit T, Fürst DO: Differential involvement of sarcomeric proteins in myofibrillar myopathies: a morphological and immunohistochemical study. Acta Neuropathol 2009, 117:293–307
37. Olivé M: Extralysosomal protein degradation in myofibrillar myopathies. Brain Pathol 2009, 19:507–515
38. Janué A, Olivé M, Ferrer I: Oxidative stress in desminopathies and myotilinopathies: a link between oxidative damage and abnormal protein aggregation. Brain Pathol 2007, 17:377–388
39. Fink AL: Protein aggregation: folding aggregates, inclusion bodies and amyloid. Fold Des 1998, 3:R9–R23
40. Kopito RR: Aggresomes, inclusion bodies and protein aggregation. Trends Cell Biol 2000, 10:524–530
41. Ross CA, Poirier MA: Protein aggregation and neurodegenerative disease. Nat Med 2004, 10:S10–S17
42. von Nandelstadh P, Soliymani R, Baumann M, Carpen O: Analysis of myotilin turnover provides mechanistic insight into the role of myotilinopathy-causing mutations. Biochem J 2011, 436:113–121
43. Goldfarb LG, Vicart P, Goebel HH, Dalakas MC: Desmin myopathy. Brain 2004, 127:723–734
44. Vicart P, Caron A, Guicheney P, Li Z, Prévost MC, Faure A, Chateau D, Chapon F, Tomé F, Dupret JM, Paulin D, Fardeau M: A missense mutation in the alphaB-crystallin chaperone gene causes a desmin-related myopathy. Nat Genet 1998, 20:92–95
45. Selcen D, Muntoni F, Burton BK, Pegoraro E, Sewry C, Bite AV, Engel AG: Mutation in BAG3 causes severe dominant childhood muscular dystrophy. Ann Neurol 2009, 65:83–89
46. Sharma S, Mücke N, Katus HA, Herrmann H, Bär H: Disease mutations in the "head" domain of the extra-sarcomeric protein desmin distinctly alter its assembly and network-forming properties. J Mol Med (Berl) 2009, 87:1207–1219
47. Bär H, Kostareva A, Sjöberg G, Sejersen T, Katus HA, Herrmann H: Forced expression of desmin and desmin mutants in cultured cells: impact of myopathic missense mutations in the central coiled-coil domain on network formation. Exp Cell Res 2006, 312:1554–1565
48. Bova MP, Yaron O, Huang Q, Ding L, Haley DA, Stewart PL, Horwitz J: Mutation R120G in alphaB-crystallin, which is linked to a desmin-related myopathy, results in an irregular structure and defective chaperone-like function. Proc Natl Acad Sci USA 1999, 96:6137–6142
49. Mologni L, Moza M, Lalowski MM, Carpén O: Characterization of mouse myotilin and its promoter. Biochem Biophys Res Commun 2005, 329:1001–1009

別冊日本臨牀　新領域別症候群シリーズ　No.20　(2012年12月20日発行) 別刷

先天代謝異常症候群(第2版) 下

—病因・病態研究，診断・治療の進歩—

XIV　結合組織異常

ベスレムミオパチーとウルリッヒ病

米川貴博
西野一三

ベスレムミオパチーとウルリッヒ病

Collagen VI related myopathy—Bethlem myopathy and Ullrich disease

Key words：COL6関連筋疾患，VI型コラーゲン，関節拘縮，側弯症，呼吸不全

米川貴博
西野一三

はじめに

ベスレムミオパチー(Bethlem myopathy: BM)は，1976年Bethlemらにより報告された常染色体優性遺伝性筋疾患である[1]．緩徐に進行する近位筋優位の筋力低下と筋萎縮に加え，比較的早期から手指・肘関節・足関節などの屈曲拘縮が出現することを特徴とする．VI型コラーゲン(COL6)をコードする*COL6A1*，*COL6A2*，*COL6A3*遺伝子のいずれかの変異により発症する．ウルリッヒ病(ウルリッヒ型先天性筋ジストロフィー(Ullrich congenital muscular dystrophy: UCMD))は，1930年Ullrichにより報告された先天性筋ジストロフィー(congenital muscular dystrophy: CMD)である[2]．常染色体劣性遺伝性または孤発性の筋疾患であり，BMと同じ遺伝子の変異により起こるがもっと重症型である．生下時からの斜頸，側弯症，近位関節拘縮を伴い，遠位関節過伸展，著明な近位筋の筋力低下，横隔膜罹患，呼吸不全の早期発症が特徴である．以前，これらは独立した別の疾患と考えられていたが，同じ遺伝子の変異により発症することから，最近ではCOL6関連筋疾患としてとらえられている．

著者らは，平成22年度厚生労働科学研究費補助金難治性疾患克服研究事業において'ベスレムミオパチーとその類縁疾患の実態調査'(以下西野班)を行った．本稿では，全国調査結果を含めたBMとUCMDの臨床的特徴や自然経過，分子病態や治療研究の進歩について紹介する．

1. 疫　学

英国では，BMの有病率0.77(10万対)に比しUCMDは0.13(10万対)であり，BMの方が高頻度である[3]．1978-2004年までの国立精神・神経医療研究センターでの筋病理および遺伝子診断実績に基づくUCMD患者頻度は0.4-0.8(10万対)と推定され，福山型先天性筋ジストロフィーについで頻度の高いCMDであった[4]．一方，BMはUCMDの1/10程度の例しかなく，BMの報告例は極めて少なかった．BMは，後述の肢帯型筋ジストロフィー(limb girdle muscular dystrophy: LGMD)として経過観察されている可能性もあり，実際にはもっと多いと推察される．

2. 病因・病態

BMあるいはUCMDの原因として，100種類以上のCOL6遺伝子変異が報告されている．BMでは大部分が優性変異であり，その多くは，Gly-Xaa-Yaaの繰り返し構造からなるtriple helical domainのN末端側のグリシンのミスセンス変異である．グリシンの変異によりCOL6の3鎖構造が障害され不完全なタンパクが産生される．triple herical domainの同じようなグリシンのミスセンス変異でも，COL6のアッセンブリーに関与する部位かどうかにより，COL6タンパク量および臨床像が異なることが知られている．最近，*COL6A2*のナンセンス変異とミスセンス変異の複合ヘテロ接合型変異による劣

Takahiro Yonekawa, Ichizo Nishino: Department of Neuromuscular Research, National Institute of Neuroscience, National Center of Neurology and Psychiatry　独立行政法人国立精神・神経医療研究センター神経研究所 疾病研究第一部

0047-1852/12/¥60/頁/JCOPY

性遺伝形式を呈するBM例も報告されている[5,6]. また, 劣性遺伝のUCMD変異の多くはナンセンス変異であり, ホモ接合型変異よりも複合ヘテロ接合型変異例が多い. UCMDの優性変異は, スプライスサイトの変異などによるin-frame欠失を伴うものが多い. 以前は, UCMD症例の大部分は, COL6遺伝子のホモあるいは複合ヘテロ接合型変異により生じると考えられていたが, 最近では*de novo*の優性変異が劣性遺伝と同じかそれ以上の頻度でみられると考えられている.

3. 診断と鑑別診断

1) 臨床症状

Bethlemらにより報告された家系の発症年齢は5歳であったが[1], その後の報告例の大部分は10-20歳発症である. 緩徐進行性の近位筋優位の筋力低下に加え, 肩甲帯, 上腕, 下腿に筋萎縮がみられやすい. 早期から関節拘縮を伴い, 指節間関節, 肘関節, 足関節の屈曲拘縮はほぼ全例に認められる. 顔面筋, 外眼筋, 咽頭筋群は侵されないが, 呼吸筋は重症例では侵されることがある. 全国調査では, 2家系8例のBM例のうち6例に足関節尖足拘縮がみられた. 発症時期は幼小児期3例, 思春期1例, 40歳頃1例(不明1例), 5例にアキレス腱延長術の既往があり, 手術時年齢は6, 10, 13, 14, 15歳であった. 早期からのつま先歩行やアキレス腱延長術の既往は診断の一助となる.

UCMDでは, 新生児期に筋緊張低下や脊柱後弯, 近位関節拘縮, 斜頸, 股関節脱臼をみる. また, 遠位関節過伸展や踵骨突出もみられる. 知能は正常である. 全身性筋力低下のため運動発達は遅延する. 全国調査では, 新生児期にフロッピーインファント47%(n=32), 哺乳不良42%(n=32), 先天性股関節脱臼36%(n=33), 斜頸27%(n=33), 多発関節拘縮20%(n=25)が認められた. 診断時年齢3.2±2.0歳での高頻度な身体所見は, 遠位関節過伸展84%(n=25), 踵の突出78%(n=23), 高口蓋66%(n=29), 近位関節拘縮55%(n=31), 側弯症54%(n=26), rigid spine 41%(n=27)であった. 独座は全例で獲得され, 独歩は78%の例で獲得された(n=32, 1.7±0.5歳).

表1に西野班において作成されたBMおよびUCMDの診断基準を示す. 実際には, 発症年齢や身体症状で病型を明確に区別することが困難な例も存在する. COL6関連筋疾患は, 重症型のUCMDと軽症型のBMを両端とする一連のスペクトラムからなると考えると理解しやすい.

2) 検査所見

CK値は, 両疾患とも正常か正常上限の数倍程度の上昇を認める. 全国調査のUCMD典型例の診断時CK値は315±108IU/Lであった. 神経伝導検査は正常であり, 針筋電図は筋原性変化を認める. 大腿部骨格筋MRI所見として, BMでは外側広筋の周辺部から障害される傾向が, UCMDではびまん性に障害されるが縫工筋, 薄筋, 長内転筋は比較的保たれることが報告されている[7].

3) 筋病理

BMでは, 筋線維の大小不同, 中心核の増加, 筋内鞘の結合織増生などの非特異的変化が主体である. 筋内鞘や基底膜の免疫組織化学では, 通常COL6の染色性は保たれており, ごくまれに異常がみられることがある.

UCMDでは, 軽度の筋原性変化からdystrophicな変化まで様々である. 筋線維の大小不同, 筋内鞘の結合織増生が認められる(図1-a). 早期UCMDでは, タイプ1線維萎縮とタイプ1線維優位からなる筋線維タイプ不均等をみる[8]. 進行例では, 極めて小径の筋線維と結合織増生が目立ち壊死線維は乏しい. COL6は, 正常対照に対し完全に欠損(complete deficiency: CD)または低下し(図1-b, c), 筋線維鞘特異的欠損(sarcolemma specific collagen VI deficiency: SSCD)も報告されている(図1-d)[9]. 我が国では, CDよりもSSCDを呈する例が85%を占める[4].

4) 鑑別診断

BMの鑑別疾患には, Emery-Dreifuss型筋ジストロフィー(Emery-Dreifuss muscular dystrophy: EDMD), LGMDがある. EDMDでは, 拡張型心筋症を伴う心伝導障害が特徴であるが,

表1-a　ベスレムミオパチーとその類縁疾患の実態調査

診断に有用な特徴	A. 臨床的特徴 a. 常染色体優性遺伝または孤発性．稀に常染色体劣性遺伝の例がある b. 主に小児期発症(通常2-5歳)．稀に成人発症例がある c. 緩徐進行性の体幹・四肢近位筋優位の筋力低下および筋萎縮 d. 早期からの関節屈曲拘縮(第II V指指節間関節．肘関節．足関節) (参考所見) ・50歳以降に歩行不能となる例が多い ・斜頸をしばしば合併する ・CK値は正常から軽度高値(1,500 IU/L以下) ・針筋電図で筋原性変化 ・心筋症や不整脈などの心合併症を欠く B. 筋生検所見 a. 筋内鞘間質増生を伴う慢性筋原性変化 b. 免疫染色でCollagen VI異常(筋線維鞘特異的欠損や部分欠損)を認めることがある C. 遺伝学的検査 a. *COL6A1*．*COL6A2*．*COL6A3*遺伝子のヘテロ接合型変異(稀にホモ接合型または複合ヘテロ接合型変異のことがある)
除外すべき疾患	早期より関節拘縮を来す筋疾患(Emery-Dreifuss型筋ジストロフィーなど)
診断カテゴリー	確実例　A+Cを満たすもの 疑い例　A+Bを満たすもの

(厚生労働科学研究費補助金　難治性疾患克服研究事業　ベスレムミオパチーとその類縁疾患の実態調査　西野班(H22-難治-一般-024)より引用)

表1-b　ウルリッヒ病(MIM# 254090．Ullrich disease．Congenital atonic-sclerotic muscular dystrophy)

診断に有用な特徴	A. 臨床的特徴 a. 常染色体劣性遺伝または孤発性 b. 生下時または乳児期発症 c. 緩徐進行性の全般性筋力低下．筋緊張低下．および筋萎縮 d. 近位関節拘縮(脊柱側弯・後弯．股関節・肘関節屈曲拘縮) e. 遠位関節過伸展(手関節．指節間関節．足関節．趾節間関節) (参考所見) ・しばしば認める臨床所見 先天性股関節脱臼．斜頸．皮膚過伸展．皮膚ケロイド形成．顔面筋罹患．踵骨突出．呼吸筋力低下 ・CK値は正常から軽度高値(1,500 IU/L以下) ・針筋電図で筋原性変化．心筋症や不整脈などの心合併症を欠く B. 筋生検所見 a. 筋内鞘間質増生を伴う慢性筋原性変化 b. 免疫染色でCollagen VIの完全欠損．筋線維鞘特異的欠損．または部分欠損 C. 遺伝学的検査 a. *COL6A1*．*COL6A2*．*COL6A3*遺伝子のホモ接合型または複合ヘテロ接合型変異またはヘテロ接合型変異
除外すべき疾患	早期より関節拘縮を来す筋疾患(Emery-Dreifuss型筋ジストロフィーなど)
診断カテゴリー	確実例　A+B+Cを満たすもの 疑い例　A+Bを満たすもの

(厚生労働科学研究費補助金　難治性疾患克服研究事業　ベスレムミオパチーとその類縁疾患の実態調査　西野班(H22-難治-一般-024)より引用)

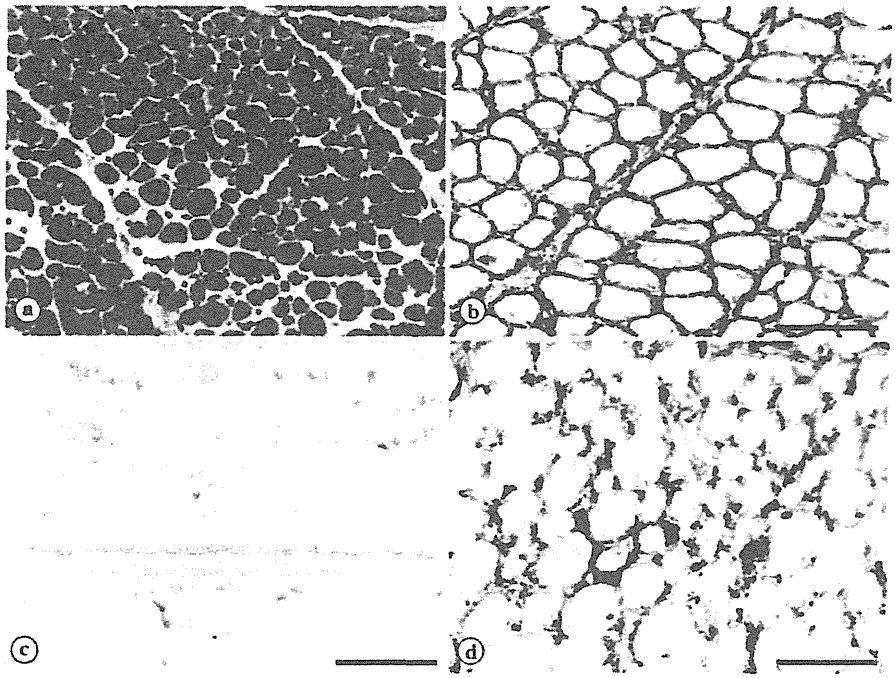

図1-a UCMDの筋病理(ヘマトキシリン・エオジン染色)
筋線維の大小不同を認める．壊死再生を伴わず，中等度の筋内鞘の結合織増生が認められる．bar=50 μm.

-b COL6の抗体染色(正常対照)
筋内鞘や周鞘，筋線維膜が染色されている．bar=50 μm.

-c COL6の抗体染色(完全欠損例)
筋線維膜だけでなく，筋内鞘や周鞘も全く染色されない．bar=50 μm.

-d COL6の抗体染色(筋線維鞘特異的欠損例)
筋内鞘にはCOL6が存在するが染色性にはむらがあり，筋線維膜では染色性が失われている．bar=50 μm.

BMではみられない．EDMDの筋力低下は上腕下腿から起こるが，BMでは肢帯あるいは全身性である．LGMDは，関節拘縮を除けばBMと同じ臨床像である．

UCMDの鑑別疾患には，他のCMD，先天性ミオパチー，脊髄性筋萎縮症，結合織疾患がある．一般に，他のCMDで遠位関節過伸展はなく，CK値もUCMDより高値である．rigid spine muscular dystrophyの経過はUCMDと似るが，歩行能力は成人期まで保たれる．早期からspinal rigidityと側弯症を含む関節拘縮を伴い，呼吸障害が出現することもUCMDと似る．EDMDでは，早期から肘関節，足関節，頸椎の関節拘縮をきたすことが特徴である．EDMDでは心筋障害がみられるがUCMDではみられない．脊髄性筋萎縮症では舌の線維束性攣縮が特徴的であり，針筋電図は神経原性変化を示す．結合織疾患では筋力低下や筋病理変化を伴わない．

4. 予後と最近の治療研究

2/3のBM患者は50歳以上まで車椅子を必要としない．実際，全国調査での2家系7例は動揺性ながら独歩可能であり，そのうち3例の年

齢は50，51，53歳であった．歩行困難の主な原因は筋力低下ではなく関節拘縮である症例が多く，リハビリテーションや整形外科的治療により歩行期間が延長しQOLが改善する可能性がある．

全国調査によれば，UCMD患者の歩行不能年齢は8.8±2.9歳(n=11)であった．vital capacityは指数的減衰を示し，10歳以前の減少が顕著であった．non-invasive ventilation導入年齢は11.2±3.6歳(n=13)であり，その年齢での%VCは36%程度であった．また，15歳未満で経年的Cobb角評価が可能な10例の年間最大増は17°(年齢9.1±2.0歳)であり，UCMDでは9歳前後数年の比較的年少の期間に側弯症が著しく増悪する．生命予後の観点からは呼吸障害の早期発見と治療が最も重要であり，定期的な呼吸機能評価や夜間経皮CO_2モニタリングに加え，関節拘縮や脊柱変形予防のリハビリテーションも重要である．

現在両疾患に有効な治療法はない．しかし，*col6a1*ノックアウトマウスや患者由来筋芽細胞においてミトコンドリア機能異常が報告されミトコンドリアmembrane permeability transition pore(PTP)開口阻害薬であるシクロスポリンAがミトコンドリア異常やアポトーシスの出現を抑制することが報告されている[10,11]．更に，オープンパイロット試験でシクロスポリンA経口投与によって病理変化が改善することも報告されている[12]．また，*col6a1*ノックアウトマウスでオートファジー機能の障害がみられること，ラパマイシンなどによってオートファジーを亢進させると筋萎縮が抑制されることも報告された[13]．オートファジー機能の改善は，COL6関連筋疾患の治療戦略として注目されている．

謝辞　本研究は，厚生労働科学研究費補助金難治性疾患等克服研究事業(難治性疾患克服研究事業)の助成を受けたものである．

文　献

1) Bethlem J, van Wijnaarden GK: Benign myopathy, with autosomal dominant inheritance. A report on three degree. Brain 99: 91-100, 1976.
2) Ullrich O: Kongenitale atonisch-skelerotische Muskeldystrophie ein weiterer Typus der heredodegenerativen Erkrankungen des neuromuskularen Systems. Z Ges Neurol Psychiat 126: 171-201, 1930.
3) Norwood FLM, et al: Prevalence of genetic muscle disease in Northern England: in depth analysis of a muscle clinic population. Brain 132: 3175-3186, 2009.
4) Okada M, et al: Primary collagen VI deficiency is the second most common congenital muscular dystrophy in Japan. Neurology 69: 1035-1042, 2007.
5) Gualandi F, et al: Autosomal recessive Bethlem myopathy. Neurology 73: 1883-1891, 2009.
6) Foley AR, et al: Autosomal recessive inheritance of classic Bethlem myopathy. Neuromuscul Disord 19: 813-817, 2009.
7) Mercuri E, et al: Muscle MRI in Ullrich congenital muscular dystrophy and Bethlem myopathy. Neuromuscul Disord 15: 303-310, 2005.
8) Schess J, et al: Predominant fiber atrophy and fiber type disproportion in early Ullrich disease. Muscle Nerve 38: 1184-1191, 2008.
9) Ishikawa H, et al: Ullrich disease due to deficiency of collagen VI in the sarcolemma. Neurology 62: 620-623, 2004.
10) Irwin WA, et al: Mitochondrial dysfunction and apoptosis in myopathic mice with collagen VI deficiency. Nat Genet 35: 367-371, 2003.
11) Angelin A, et al: Mitochondrial dysfunction in the pathogenesis of Ullrich congenital muscular dystrophy and prospective theraphy with cyclosporins. Proc Natl Acad Sci USA 104: 991-996, 2007.
12) Merlini L, et al: Cyclosporin A corrects mitochondrial dysfunction and muscle apoptosis in patients with collagen VI myopathies. Proc Natl Acad Sci USA 105: 5225-5229, 2008.
13) Grumati P, et al: Autophagy is defective in collagen VI muscular dystrophies, and its reactivation rescues myofiber degeneration. Nat Med 16: 1313-1320, 2010.